

## The AEGIS experiment at CERN: measuring antihydrogen free-fall in earth's gravitational field to test WEP with antimatter

This content has been downloaded from IOPscience. Please scroll down to see the full text.

2017 J. Phys.: Conf. Ser. 791 012014

(<http://iopscience.iop.org/1742-6596/791/1/012014>)

View [the table of contents for this issue](#), or go to the [journal homepage](#) for more

Download details:

IP Address: 192.167.18.242

This content was downloaded on 20/05/2017 at 21:51

Please note that [terms and conditions apply](#).

You may also be interested in:

[Prospects for measuring the gravitational free-fall of antihydrogen with emulsion detectors](#)

S Aghion, O Ahlén, C Amsler et al.

[Particle tracking at cryogenic temperatures: the Fast Annihilation Cryogenic Tracking \(FACT\) detector for the AEGIS antimatter gravity experiment](#)

J. Storey, S. Aghion, C. Amsler et al.

[A new application of emulsions to measure the gravitational force on antihydrogen](#)

C Amsler, A Ariga, T Ariga et al.

[AEGIS: An experiment to measure the gravitational interaction between matter and antimatter](#)

Michael Doser and the Aegis collaboration

[Exploring the WEP with a pulsed cold beam of antihydrogen](#)

M Doser, C Amsler, A Belov et al.

[Production and thermalization of positronium in homogeneous porous silica](#)

S Aghion, R Ferragut, F Moia et al.

[Homogeneous porous silica for positronium production in AEGIS](#)

R Ferragut, A Dupasquier, A Calloni et al.

[CERN opens antimatter factory](#)

Richard Hendricks

[Positronium formation in porous materials for antihydrogen production](#)

R Ferragut, A Calloni, A Dupasquier et al.

# The AEGIS experiment at CERN: measuring antihydrogen free- fall in earth's gravitational field to test WEP with antimatter

R S Brusa<sup>1,2</sup>, C Amsler<sup>3</sup>, T Ariga<sup>3</sup>, G Bonomi<sup>4,5</sup>, P Bräunig<sup>6</sup>, L Cabaret<sup>7</sup>, M Caccia<sup>8,9</sup>, R Caravita<sup>10,11</sup>, F Castelli<sup>8,12</sup>, G Cerchiari<sup>13</sup>, D Comparat<sup>7</sup>, G Consolati<sup>8,14</sup>, A. Demetrio<sup>6</sup>, L Di Noto<sup>10,11</sup>, M Doser<sup>15</sup>, A Ereditato<sup>3</sup>, C Evans<sup>8,14</sup>, R Ferragut<sup>8,14</sup>, J Fesel<sup>15</sup>, A Fontana<sup>5</sup>, S Gerber<sup>15</sup>, M Giammarchi<sup>8</sup>, A Gligorova<sup>16</sup>, F Guatieri<sup>1,2</sup>, S Haider<sup>15</sup>, H Holmestad<sup>17</sup>, T Huse<sup>17</sup>, A Kellerbauer<sup>13</sup>, D Krasnický<sup>10,11</sup>, V Lagomarsino<sup>10,11</sup>, P Lansonneur<sup>18</sup>, P Lebrun<sup>18</sup>, C Malbrunot<sup>15,19</sup>, S Mariazzi<sup>19</sup>, V Matveev<sup>20,21</sup>, Z Mazzotta<sup>8,12</sup>, G Nebbia<sup>22</sup>, P Nedelec<sup>18</sup>, M Oberthaler<sup>6</sup>, N Pacifico<sup>16</sup>, D Pagano<sup>4,5</sup>, L Penasa<sup>1,2</sup>, V Petracek<sup>23</sup>, C Pistillo<sup>3</sup>, F Prelz<sup>8</sup>, M Prevedelli<sup>24</sup>, L Ravelli<sup>1,2</sup>, B Rienaecker<sup>15</sup>, O M Röhne<sup>17</sup>, A Rotondi<sup>5,25</sup>, M Sacerdoti<sup>8,12</sup>, H Sandaker<sup>17</sup>, R Santoro<sup>8,9</sup>, P Scampoli<sup>3,26</sup>, L Smestad<sup>15,27</sup>, F Sorrentino<sup>10,11</sup>, I M Strojek<sup>18</sup>, G Testera<sup>11</sup>, I C Tietje<sup>15</sup>, S Vamosi<sup>19</sup>, E Widmann<sup>19</sup>, P Yzombard<sup>7</sup>, J Zmeskal<sup>19</sup> and N Zurlo<sup>5,28</sup>

<sup>1</sup> Department of Physics, University of Trento, via Sommarive 14, 38123 Povo, Trento, Italy

<sup>2</sup> TIFPA/INFN Trento, via Sommarive 14, 38123 Povo, Trento, Italy

<sup>3</sup> Laboratory for High Energy Physics, Albert Einstein Center for Fundamental Physics, University of Bern, 3012 Bern, Switzerland

<sup>4</sup> Department of Mechanical and Industrial Engineering, University of Brescia, via Branze 38, 25123 Brescia, Italy

<sup>5</sup> INFN Pavia, via Bassi 6, 2790 Pavia, Italy

<sup>6</sup> Kirchhoff-Institute for Physics, Heidelberg University, Im Neuenheimer Feld 227, 68120 Heidelberg, Germany

<sup>7</sup> Laboratoire Aimé Cotton, Université Paris-Sud, ENS Cachan, CNRS, Université Paris-Saclay, 91405 Orsay Cedex, France

<sup>8</sup> INFN Milano, via Celoria 16, 20133 Milano, Italy

<sup>9</sup> Department of Science, University of Insubria, Via Valleggio 11, 2290 Como, Italy

<sup>10</sup> Department of Physics, University of Genova, via Dodecaneso 33, 16146 Genova, Italy

<sup>11</sup> INFN Genova, via Dodecaneso 33, 16146 Genova, Italy

<sup>12</sup> Department of Physics, University of Milano, via Celoria 16, 20133 Milano, Italy

<sup>13</sup> Max Planck Institute for Nuclear Physics, Saupfercheckweg 1, 68117 Heidelberg, Germany

<sup>14</sup> Politecnico of Milano, Piazza Leonardo da Vinci 32, 20133 Milano, Italy

<sup>15</sup> Physics Department, CERN, 1211 Geneva 23, Switzerland



<sup>16</sup> Institute of Physics and Technology, University of Bergen, Allégaten 55, 5007 Bergen, Norway

<sup>17</sup> Department of Physics, University of Oslo, Sem Sælandsvei 24, 0371 Oslo, Norway

<sup>18</sup> Institute of Nuclear Physics, CNRS/IN2p3, University of Lyon 1, 68622 Villeurbanne, France

<sup>19</sup> Stefan Meyer Institute for Subatomic Physics, Austrian Academy of Sciences, Boltzmannngasse 3, 980 Vienna, Austria

<sup>20</sup> Institute for Nuclear Research of the Russian Academy of Science, Moscow 117312, Russia

<sup>21</sup> Joint Institute for Nuclear Research, 141980 Dubna, Russia

<sup>22</sup> INFN Padova, via Marzolo 8, 35131 Padova, Italy

<sup>23</sup> Czech Technical University, Prague, Břehová 7, 11518 Prague 1, Czech Republic

<sup>24</sup> University of Bologna, Viale Berti Pichat 6/2, 40126 Bologna, Italy

<sup>25</sup> Department of Physics, University of Pavia, via Bassi 6, 2790 Pavia, Italy

<sup>26</sup> Department of Physics “Ettore Pancini”, University of Napoli Federico II, Complesso Universitario di Monte S. Angelo, 80126, Napoli, Italy

<sup>27</sup> The Research Council of Norway, P.O. Box 564, NO-1327 Lysaker, Norway

<sup>28</sup> Department of Civil Engineering, University of Brescia, via Branze 43, 25123 Brescia, Italy

E-mail: brusa@science.unitn.it

**Abstract.** The AEgIS (Antimatter Experiment: Gravity, Interferometry, Spectroscopy) experiment is designed with the objective to test the weak equivalence principle with antimatter by studying the free fall of antihydrogen in the Earth’s gravitational field. A pulsed cold beam of antihydrogen will be produced by charge exchange between cold Ps excited in Rydberg state and cold antiprotons. Finally the free fall will be measured by a classical moiré deflectometer. The apparatus being assembled at the Antiproton Decelerator at CERN will be described, then the advancements of the experiment will be reported: positrons and antiprotons trapping measurements, Ps two-step excitation and a test-measurement of antiprotons deflection with a small scale moiré deflectometer.

## 1. Introduction

The weak equivalence principle (WEP), also known as universality of free fall (UFF), states that in a gravitational field all bodies, irrespective of their mass and composition, fall with the same acceleration. UFF of matter in the field of Earth has been tested by measuring the dimensionless parameter  $\eta = \Delta a/a$  where  $\Delta a$  is the relative acceleration between two proof masses as they fall with an acceleration  $a$  towards the Earth; validity of UFF-WEP requires  $\eta = 0$ . Precision experiments with torsion balance and dropping of cold-atoms have measured  $\eta$  reaching values of  $\cong 10^{-13}$  and  $\cong 10^{-7}$ , respectively [1]. Up to now, in spite of very precise experiments done with matter, none has been carried out to test UFF-WEP with antimatter.

The AEgIS experiment, set up at the Antiproton Decelerator (AD) at CERN, is designed with the primary scientific goal of measuring for the first time the free fall of antihydrogen ( $\bar{H}$ ) in the Earth’s gravitational field with percent order precision [2]. In the experiment, the measurement of the gravitational acceleration  $\bar{g}$  on  $\bar{H}$  will be carried out by measuring the time of flight and the vertical displacement of each  $\bar{H}$  after its passage through a moiré deflectometer realized with two gratings and

a position sensitive detector. The needed pulsed cold beam of  $\bar{H}$  will be produced by charge exchange among excited Ps atoms and cooled antiprotons.

In this paper the current progress towards forming a cold antihydrogen beam and measuring gravity will be summarized.

## 2. The AEgIS experiment: method and set-up

A detailed description of the experiment can be found in [3]. The method proposed by AEgIS to form a cold  $\bar{H}$  beam is sketched in Figure 1. Bunches of more than  $10^8$  positrons with a duration of about 10 ns are shot on a positron-positronium (Ps) converter. Collisionally cooled Ps emitted into vacuum is excited in Rydberg states. These long living Ps fly into the antiproton trap, where  $\bar{H}$  can be formed in an excited state by the charge exchange reaction:  $Ps^* + \bar{p} \rightarrow \bar{H}^* + e^-$ . Ps excitation in high Rydberg states is necessary not only to lengthen its lifetime, but also to augment the  $\bar{H}^*$  yield: the cross section of the charge exchange reaction is proportional to  $n^4$  where  $n$  is the Ps principal quantum number. Finally, excited  $\bar{H}^*$  are Stark accelerated towards a moiré deflectometer, the classical analogue of a matter wave interferometer. Along its travel  $\bar{H}^*$  decays to ground state.

A sketch of the moiré deflectometer is shown in the right panel of Figure 1. The present design, details reported in Ref. [3], is based on a device previously used to measure the gravity acceleration of an argon beam with high sensitivity [4].

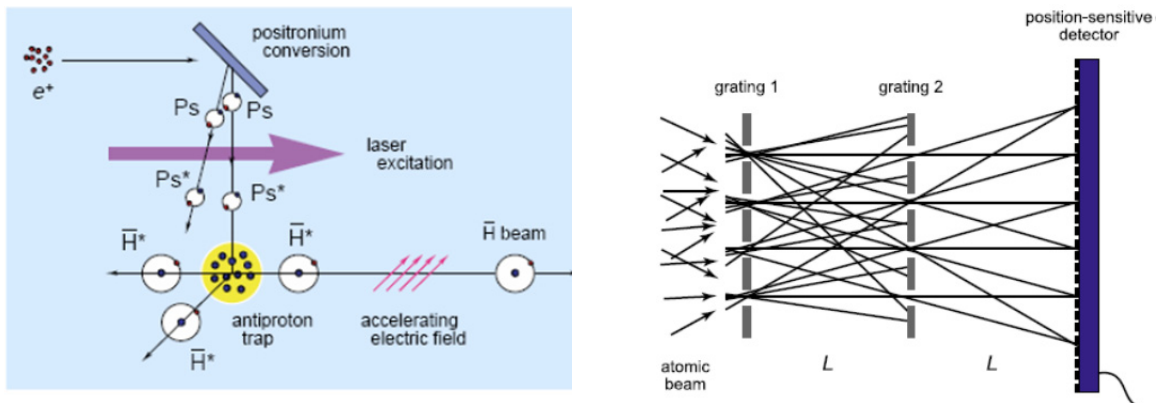


**Figure 1.** Left, the AEgIS method for the production of a pulsed cold  $\bar{H}$  beam. Right, sketch illustrating the moiré deflectometer technique [3, 4]. A divergent  $\bar{H}$  beam ( $v \sim 400 - 600 \text{ m s}^{-1}$ ) propagates through two identical gratings with a period equal to the grating period ( $80 \mu\text{m}$ ) at a distance  $L=40 \text{ cm}$ .  $\bar{H}$  passing the gratings follow a parabolic path and annihilate on a position sensitive detector with a downward shift that would be of the order of  $10 \mu\text{m}$  considering an acting gravitational force as on a H atom.

The experimental apparatus scheme is shown in Figure 2, details in [5]. The AD delivers bunches of  $\sim 3 \times 10^7 \bar{p}$  every  $\sim 110 \text{ s}$  with  $5.3 \text{ MeV}$  kinetic energy. Antiprotons passing through aluminium foils (degrader) are slowed down to a few keV and then caught in a  $75 \text{ cm}$  long set of Penning-Malmberg traps in the  $5 \text{ T}$  magnet. Trapped  $\bar{p}$  are cooled to a few Kelvin by sympathetic cooling with a cloud of  $10^7$ - $10^9$  electrons previously stored in a  $100$ - $150 \text{ V}$  potential well (see section 3). Cooled  $\bar{p}$  are then transferred into a second Penning-Malmberg trap in the  $1 \text{ T}$  magnet and wait there for Ps to form  $\bar{H}$ .

Positrons, from a  $^{22}\text{Na}$  radioactive source ( $\sim 10 \text{ mCi}$ ) coupled to a Ne moderator [6], are cooled in a two-stage Surko buffer trap [7] and stored in a Penning-Malmberg accumulator that releases bunches of some  $10^7 e^+$ , which are then transferred and trapped in the  $5 \text{ T}$  magnet.

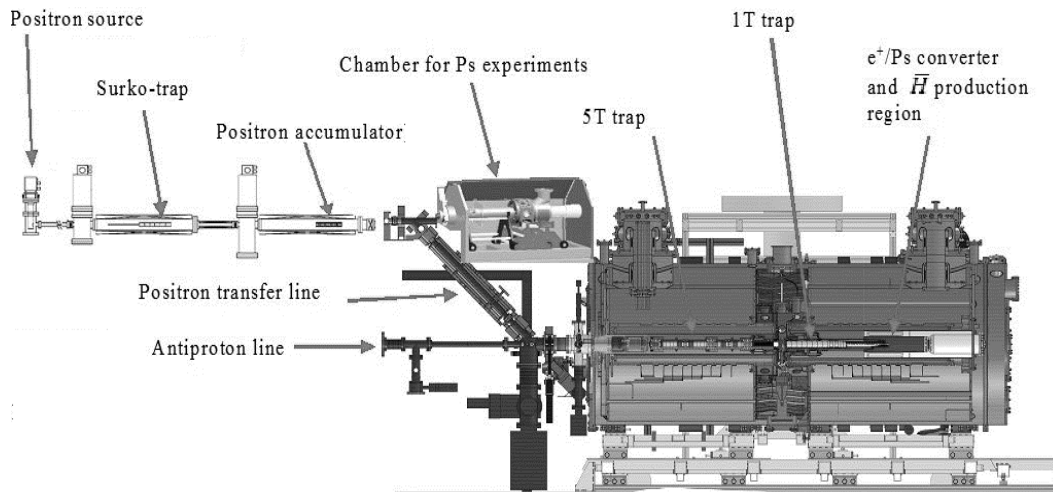


**Figure 2.** Scheme of the AEGIS experimental set-up.

*Ps* in vacuum is produced by transferring and implanting previously trapped positrons (see section 3) in a porous silica converter installed in the 1T magnet. UV ( $\lambda=205$  nm) and IR ( $\lambda\sim 1670$  nm) laser light [8] is transported with glass fibers in front of the converter to perform a two-step *Ps* excitation:  $1^3S \rightarrow 3^3P$ ,  $3^3P \rightarrow$  Rydberg states (see section 4).

In addition to the main apparatus for  $\bar{H}$  gravity study, a chamber to perform *Ps* formation and excitation experiments is connected to the accumulator through a 60 cm magnetic transport line. Positrons pass through a magnetic field terminator and are bunched ( $\sim 7$  ns FWHM) and focused on a *Ps* converter with a spot of less than 4 mm FWTM; bunched positron energy varies in the 3 to 8 keV range [9, 10].

### 3. Trapping positrons and antiprotons in the 5T magnet

A reproducible procedure for trapping  $e^+$  and  $\bar{p}$  in the 5T region was devised during the 2015 AD run [5, 11]. Bunches of  $e^+$ , with a longitudinal velocity corresponding to an energy of 300 eV, were magnetically transported in a 0.14 T field and injected into the Penning-Malmberg trap in a 4.5 T magnetic field. Positrons are cooled down by cyclotron radiation and trapped in a 50-100 eV potential well. The number of stored  $e^+$  and  $e^+$  lifetime in the trap were evaluated by dumping the particles on a stopper and measuring annihilation gamma-rays with plastic scintillators placed around the 1T-5T chamber. When  $\sim 2.5 \times 10^7$   $e^+$  are trapped, about 100% of them cool down without observed losses for storage times up to more than 30 min. Thanks to the long lifetime of  $e^+$  in the trap, it was possible to accumulate more than  $2 \times 10^8$   $e^+$ , transferring shots of  $1.8 \times 10^7$   $e^+$  from the accumulator, see left panel in Figure 3.

Study of trapped  $\bar{p}$  was done in the same Penning-Malmberg trap used to store  $e^+$ . On the average  $3.6 \times 10^5$   $\bar{p}$  were captured for each shot of  $3.0 \times 10^7$   $\bar{p}$  delivered by AD, with an optimized 9 kV trapping potential. Before capturing  $\bar{p}$ , the trap was loaded with  $10^7$ - $10^9$  electrons for  $\bar{p}$  electron-cooling. The remaining hot fraction of  $\bar{p}$  was firstly ejected by lowering the trapping high-voltage to a low-voltage (fraction HD-hot dump). Then the cooled fraction was dumped by lowering the low-voltage (fraction CD-cold dump). In Fig. 3, right panel, the fraction of cooled  $\bar{p}$  (CD) against the total trapped  $\bar{p}$  (CD+HD) is reported as a function of the time spent by  $\bar{p}$  with electrons. A cooling efficiency of 90% was achieved in about 60 s with an optimum overlap of the  $e^-$  -  $\bar{p}$  clouds.

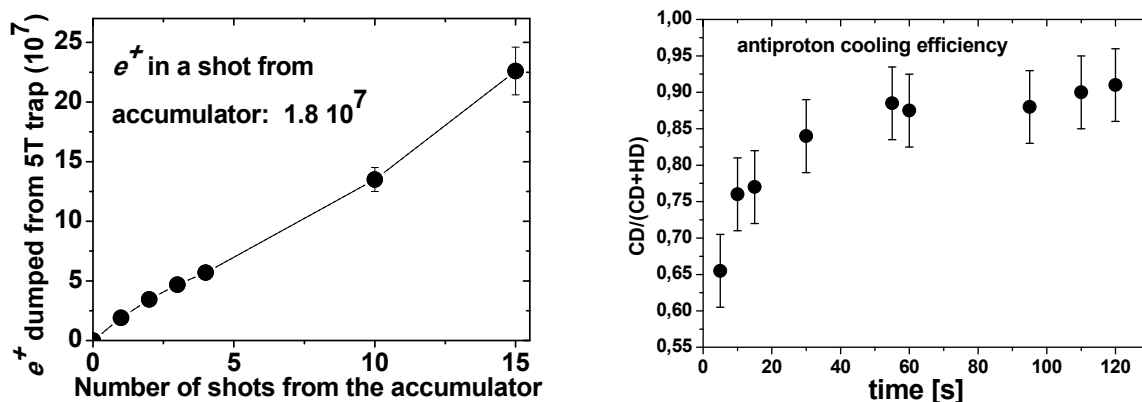


**Figure 3.** Left: Trapped  $e^+$  in the 5T region as a function of number of shots from the accumulator; errors are statistical and due to the fluctuation in the number of  $e^+$  from the accumulator. Right: fraction of cold  $\bar{p}$  as a function of time spent in the trap with electrons; errors are the statistical and due to fluctuation in the number of  $\bar{p}$  delivered by AD. Reproduced from Ref. [5] and Ref. [11].

#### 4. Positronium formation and excitation in the secondary chamber

$Ps$  formation, emission into vacuum and excitation in Rydberg states were proved and verified in the “chamber for  $Ps$  experiments” [10] in line with the Surko trap and the accumulator, see Figure 2.

High yield of  $Ps$  in vacuum was observed [10] using a Si target with oriented oxidized nanochannels [12, 13] as  $e^+/Ps$  converters.  $Ps$  excitation was measured by the SSPALS (Single Shot Positron Annihilation Lifetime Spectroscopy) method firstly introduced by Cassidy and Mills [14] to study two-step,  $1^3S \rightarrow 2^3P$ ,  $2^3P \rightarrow$  Rydberg excitation [15],  $Ps$ - $Ps$  interaction [16] and to observe  $Ps_2$  molecules [17].

The lifetime spectra from the single gamma ray shots were acquired with a  $PbWO_4$  scintillator coupled to a Hamamatsu R11265-100 photomultiplier tube. A laser system to perform the two-step  $Ps$  excitation  $1^3S \rightarrow 3^3P$ ,  $3^3P \rightarrow$  Rydberg was designed and set up [8].

A UV laser pulse (205 nm, energy 54  $\mu$ J, pulse width  $\sim$  1.5 ns) was used to excite  $Ps$  from ground to  $n=3$  state and simultaneously an IR laser ( $\lambda=1064$  nm, 50 mJ, 10 ns temporal pulse width) was shot to ionize the excited  $Ps$ .

An IR laser (tuneable wavelength in the  $\sim$  1650-  $\sim$ 1720 nm range, energy  $\sim$  1mJ, pulse width  $\sim$ 4 ns) was pulsed at the same time with the UV laser to excite  $Ps$  from  $n=3$  to Rydberg levels.

Results are shown in Figure 4. Experiment details and analysis of the data are extensively reported in [18].

The black lines in Figure 4, after the annihilation prompt peak, correspond to the  $Ps$  decaying in vacuum. When the UV+IR ( $\lambda=1064$  nm) lasers are shot on the  $Ps$  cloud,  $Ps$  population is decreased by the fraction of ionized  $Ps$  atoms, as shown by the grey curve in the left panel of Figure 4. The decrease is evaluated with the parameter  $S = (f_{off} - f_{on})/f_{off}$  where  $f_{off}$  and  $f_{on}$  are the areas of the SSPALS spectra between 50 and 250 ns with the laser *off* and *on*. In the inset (left panel Fig.4) the  $1^3S \rightarrow 3^3P$  excitation linewidth obtained measuring  $S\%$  as a function of the UV wavelength is shown.

The lifetime of  $Ps$ , when excited in Rydberg states, increases up to microseconds allowing  $Ps^*$  to reach the walls of the vacuum chamber. In this case the SSPALS spectrum shows a decrease of annihilations after the prompt peak due to the  $Ps^*$  formation (as shown in the grey curve up 300 ns in the right panel of Figure 4) and an increase of annihilations when  $Ps^*$  start reaching the chamber walls, as shown in the grey curve after 300 ns in the right panel of Figure 4. A scan of the IR laser wavelength, while keeping the UV laser wavelength constant on  $n=3$  resonance ( $\lambda=205.05$  nm), was

carried out to resolve the  $n=15$  Rydberg line, and partially the  $n=16-17$  lines due to the excessive broadening. The  $-S\%$  calculated between 300-600 ns is shown in the inset (right panel Figure 4) as a function of the IR wavelength.

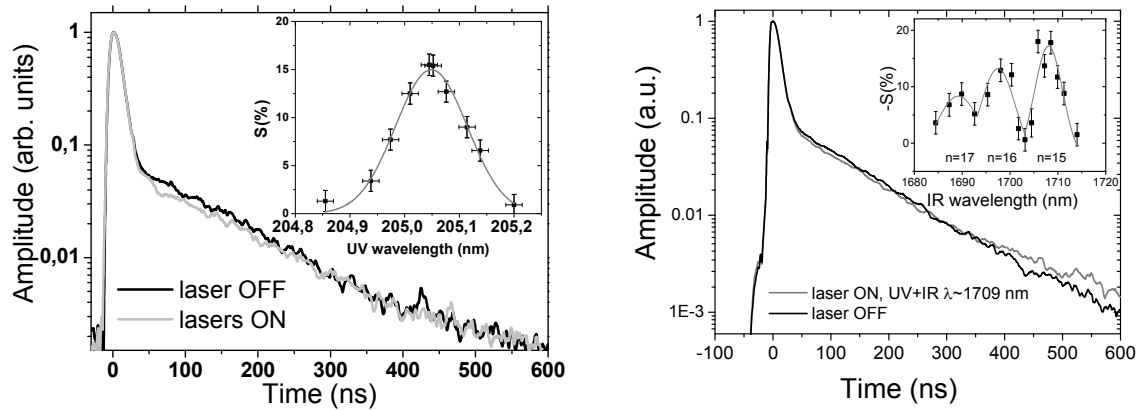


**Figure 4.** SSPALS spectra. Left:  $Ps$  in vacuum, laser off, black line; laser (UV+IR for ionization) on, grey line; the inset shows the scan of the UV wavelength, showing the  $n=3$  excitation line. Right:  $Ps$  in vacuum, laser off, black line; laser (UV+IR for excitation) on, grey line; the inset shows the scan with the IR wavelength, showing the  $Ps$  excitation in the  $n=15-17$  Rydberg states; the continuous line is for eye guide. Reproduced from Ref. 18.

### 5. Moiré deflectometer: concept proof with antiprotons

To prove the basis of the technique, a small scale moiré deflectometer was realized and tested with a beam of antiprotons with 106 keV mean energy [19]. The distance  $L$  between the gratings and the detector was set  $L=25$  mm, see Figure 1 for the scheme. The slits in the 100  $\mu\text{m}$  thick silicon grating were manufactured with a 12  $\mu\text{m}$  width and a 40  $\mu\text{m}$  periodicity, ensuring a classical regime when these dimensions are compared to the de Broglie wavelength of the antiprotons. The annihilation positions of  $\bar{p}$ , which have passed the grating, were detected by an emulsion detector [20, 21] with a 2  $\mu\text{m}$  resolution. The moiré deflectometer and the emulsion detector were mounted at the end of the two main magnets (1T and 5T, Figure 2) in a dedicated vacuum chamber. A moiré pattern of 241 antiproton annihilation events was recorded and the absolute fringe pattern shift was determined by comparing with a reference Talbot-Laue pattern obtained by illuminating the deflectometer with light. The shift is given by  $\Delta y = F\tau^2/m$ , where  $F$  is the force perpendicular to the slits,  $\tau$  is the time of flight between the two gratings and  $m$  the  $\bar{p}$  mass. The observed upward shift,  $\Delta y = 9.8 \mu\text{m} \pm 0.9 \mu\text{m}$  (stat.)  $\pm 6.4 \mu\text{m}$  (syst.) (Figure 5), was found to be consistent with a mean force of 530 aN  $\pm 50$  aN (stat.)  $\pm 350$  aN (syst.) acting on the antiprotons. This force can be caused by a magnetic field component of  $\sim 7.4$  G, compatible with a magnetic field of  $\sim 10$  G measured in the position of the deflectometer.

The gravitational force acting on a  $\bar{H}$  atom will be ten order of magnitude smaller than the force measured in this test with the small scale moiré, nevertheless this experiment proves that the detection of the fall under gravity of antihydrogen atoms can be achieved if the small moiré deflectometer is scaled for increasing the time of flight  $\tau$ . As a matter of fact, with a shift of the order of 10  $\mu\text{m}$ , a better sensitivity of 11 orders of magnitude can be reached forming a  $\bar{H}$  beam with 500 m/s velocity and increasing at 1 m the distance between the two gratings.

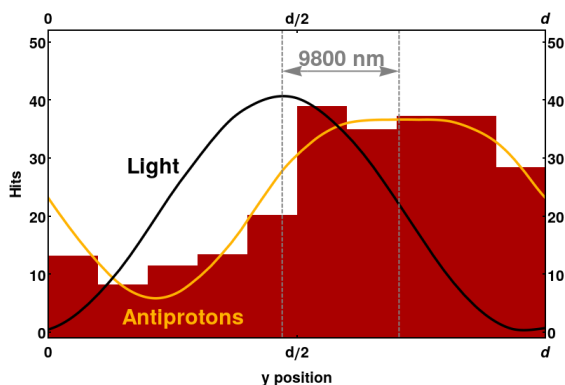


**Figure 5.** The light and  $\bar{p}$  patterns showing the observed  $\bar{p}$  shift of antiprotons with the moiré deflectometer. Reproduced from Ref. [19].

## 6. Conclusions

The design of the AEGIS experiment requires the development of several techniques: first to manipulate antiprotons, positrons and positronium for the production of an antihydrogen beam and then, to manipulate antihydrogen for studying its free fall in the Earth's gravitational field. In this paper the last achievements in this development have been reported. They can be summarized as follow.

At present, about  $3.6 \times 10^5$  antiprotons are captured per shot of antiprotons ( $3.0 \times 10^7$ ) delivered by AD and 90% of them are electron-cooled in the 4.5 T trap. Although working with a 10 mCi  $^{22}\text{Na}$  source, up to  $2.2 \times 10^8$  positrons can be routinely trapped and cooled in the 4.5 T magnet and can be there stored for tens of minutes without significant losses. With a stronger source it is expected to increase the number of trapped  $e^+$  and decrease the time to fill the trap.

A laser system was set up to perform a two-step  $1^3S \rightarrow 3^3P$ ,  $3^3P \rightarrow \text{Rydberg Ps}$  excitation: a fundamental advancement towards the antihydrogen production by the charge exchange reaction between antiprotons and excited Ps. Clouds of Ps atoms were obtained in vacuum by implanting positron bunches in an efficient  $e^+/\text{Ps}$  nanochannelled silicon converter allocated in a dedicated chamber for performing Ps experiments. Positrons from a two-stage Surko trap were transferred into an accumulator and then dumped and re-bunched on the Si converter. The excitation experiment was performed detecting the Ps excited fraction by employing the SSPALS technique.

Finally the feasibility of the free fall measurement of  $\bar{H}$  by a moiré deflectometer was proved by measuring the deflection of an antiproton beam with a small scale moiré deflectometer and an emulsion detector with 2  $\mu\text{m}$  resolution. It was shown that shift of ten microns, as expected in a free fall experiment with  $\bar{H}$ , can be effectively measured.

## References

- [1] Nobili A M 2016 *Phys. Rev. A* **93** 023617
- [2] Drobychev G et al 2007 CERN-SPSC-2007-017, <http://cdsweb.cern.ch/record/1037532>
- [3] Doser M et al. 2012 *Class. Quantum Grav.* **29** 184009
- [4] Oberthaler M K, Bernet S, Rasel E M, Schmiedmayer J and Zeilinger A 1996 *Phys. Rev. A* **54** 3165
- [5] Mariuzzi S et al. 2016 *J. Phys: Conf. Ser.* in print
- [6] Mills A P Jr and Gullikson E M 1986 *Appl. Phys. Lett.* **49** 1121
- [7] Danielson J R, Dubin D H E, Greaves R G and Surko C M 2015 *Rev. Mod. Phys.* **87** 247
- [8] Cialdi S, Boscolo I, Castelli F, Villa F, Ferrari G and Giammarchi M G 2011 *Nucl. Instrum. Methods Phys. Res. B* **269** 1527
- [9] Penasa L, Di Noto L, Bettonte M, Mariuzzi S, Nebbia G and Brusa R S 2014 *J. Phys: Conf. Ser.* **505** 012031
- [10] Aghion S et al. 2015 *Nucl. Instrum. Methods Phys. Res. B* **362** 86



- [11] Caravita R *et al.* 2016 *WAG proceeding* in print
- [12] Mariazzi S, Bettotti P, Larcheri S, Toniutti L and Brusa R S 2010 *Phys. Rev. B* **81** 235418
- [13] Mariazzi S, Bettotti P and Brusa R S 2010 *Phys. Rev. Lett.* **104** 243401
- [14] Cassidy D B, Deng S H M, Tanaka H K M and Mills A P Jr 2006 *Appl. Phys. Lett.* **88** 194105
- [15] Cassidy D B, Hisakado T H, Tom H W K and Mills A P Jr 2012 *Phys. Rev. Lett.* **108** 043401
- [16] Cassidy D B and Mills A P Jr 2008 *Phys. Rev. Lett.* **100** 013401
- [17] Cassidy D B and Mills A P Jr 2007 *Nature* **449** 195
- [18] Aghion S *et al.* 2016 *Phys. Rev. A* **94** 012507
- [19] Aghion S *et al.* 2014 *Nat. Commun.* **5** 4538
- [20] M. Kimura *et al.* 2013 *Nucl. Instrum. Methods Phys. Res. A* **732** 325
- [21] Aghion S *et al.* 2013 *JINST* **8** P08013